Improved Photovoltaic Performance of Heterostructured Tetrapod-Shaped CdSe/CdTe Nanocrystals Using C60 Interlayer

By *Yanqin Li, Rosanna Mastria, Angela Fiore, Concetta Nobile, Lunxiang Yin, Mariano Biasiucci, Gang Cheng, Anna Maria Cucolo, Roberto Cingolani, Liberato Manna,* and *Giuseppe Gigli**

Semiconductor nanocrystals (NCs) are promising building blocks for future-generation photovoltaic (PV) devices, such as all-inorganic NC solar cells,[1–3] hybrid nanocrystal–polymer composite solar cells,[4–9] and dye-sensitized solar cells.[10,11] Colloidal inorganic NCs could offer processing, scale, and cost advantages of organics, while retaining the broadband absorption and superior transport properties of traditional PV semiconductors.[12–14] Recently, considerable research has focused on the synthesis, shape control, and photophysics of heterostructured type-II nanocrystals.[15–18] Joining together in a single nanostructure two materials with a type-II band offset can induce spatial separation of photogenerated carriers within the nanostructure itself, with the electron residing in one material and the hole in the other. This capability to intrinsically dissociate photogenerated excitons[15–19] renders these nanocrystals excellent candidates for application in PV devices.[19] Our group reported recently an approach to prepare heterostructured tetrapod-shaped colloidal nanocrystals based on a CdSe core region and CdTe arms (see sketches in Fig. 2a and b).[20] These nanocrystals were synthesized using preformed seeds in the sphalerite structure, onto which hexagonal wurtzite arms were grown by coinjection of the seeds and of the chemical precursors into a hot mixture of surfactants.

The best hybrid polymer–nanocrystal PV cells in terms of efficiency have been reported by Alivisatos and Greenham using CdSe-based nanocrystals.[5–8] To date, most colloidal semiconductor nanocrystal materials have been employed as electron acceptors in hybrid PV devices. This approach, however, does not exploit the full potential of colloidal type-II tetrapod nanocrystal heterostructures, in which from one side charge separation is enhanced, but from the other side electron localization can occur in the central seed, thus preventing charge percolation to the electrodes. To overcome this problem we report here the fabrication of hybrid photovoltaic devices based on CdSe/CdTe-C60, in which the nanocrystal layer works as electron donor and C60 as electron-acceptor/transport layer. The PV performance was greatly improved with respect to that of CdSe/CdTe-poly(3-hexylthiophene-2,5-diyl) (P3HT) and only-CdSe/CdTe-based devices, fabricated as reference. The approach bases the efficacy on the excellent exciton mobility, relatively large exciton diffusion length,[21,22] and high electron affinity of C60, which acts as electron-acceptor and electron-transporting material, thus allowing for better electron percolation to the electrodes. So far, lifetime tests have not been carried out. However, as reported by Shiga et al.,[23] it was found that a C60 buffer layer provided an additional protection to oxygen and humidity, thus improving device stability. The proposed approach demonstrates the potential for the development of optimized hybrid organic–inorganic PV devices utilizing fullerene, and provides a new general method for the fabrication of hybrid nanocrystal–C60 cells with a potentially long lifetime.

In our recent approach to prepare tetrapod-shaped colloidal nanocrystals[20], we could synthesize tetrapods from various combinations of group II–VI semiconductors, and we could independently vary the chemical composition of the central core region and that of the arms. Figure 1a shows, for instance, the transmission electron microscopy (TEM) image of the spherical CdSe nanocrystal ''seeds'' onto which CdTe arms were subsequently grown. These seeds (which had sphalerite structure) had diameters of about 3 nm. Figure 1b reports a TEM image of the tetrapod-shaped CdSe/CdTe nanocrystal heterostructures characterized by narrow distributions of arm lengths and diameters. The tetrapod arms had average diameters of about 6.5 nm, and average lengths of approximately 25 nm. In the present report, CdSe/CdTe tetrapods were exploited as active materials in photovoltaic devices. Bulk CdSe/CdTe heterojunctions present a natural type-II band offset, in which the valence band and the conduction band of the CdSe are both energetically below the respective bands of CdTe,[24] and the same is found in nanocrystals. In an heterostructure such as CdSe/CdTe, light is

[*] Prof. G. Gigli, Dr. Y. Q. Li,[+] R. Mastria, A. Fiore, Dr. C. Nobile, Dr. L. X. Yin,[+] Dr. M. Biasiucci, Dr. G. Cheng, Prof. R. Cingolani, Dr. L. Manna
National Nanotechnology Lab of CNR-INFM (NNL)
University of Salento
Via Arnesano, 73100 Lecce (Italy)
E-mail: Giuseppe.gigli@unile.it
Dr. M. Biasiucci, Prof. A. M. Cucolo
Physical Department ''E. R. Caianiello''
University of Salerno
Via S. Allende, 84081 Baronissi (SA) (Italy)

[+] Current address: Chemical Department, Dalian University of Technology, Dalian, 116023, P. R. China

DOI: 10.1002/adma.200901338

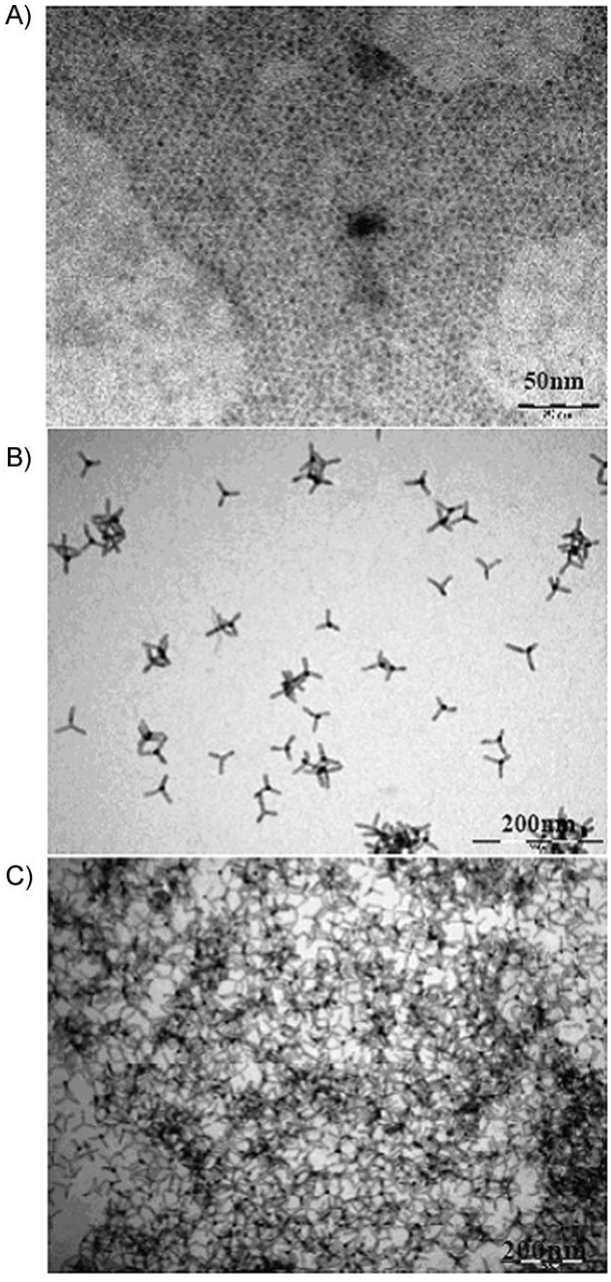

Figure 1. a) TEM image of spherical CdSe nanocrystals used as seeds for growing the tetrapods. b) TEM image of tetrapod-shaped CdSe/CdTe nanocrystals. c) Thin films of CdSe/CdTe tetrapods (89 wt%) in P3HT studied using TEM.

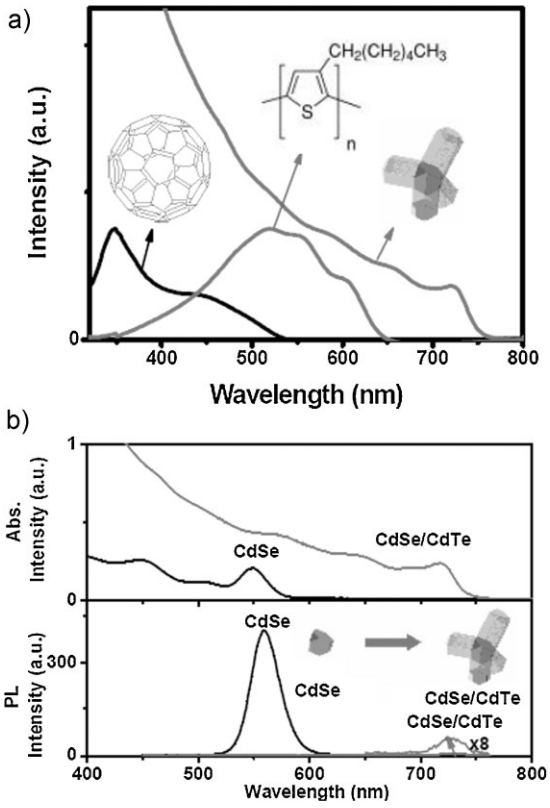

Figure 2. a) Absorption spectra and molecular structures used in the investigated photovoltaic cells. b) Absorption and PL spectra of CdSe seeds and of the CdSe/CdTe tetrapods. Sketch highlighting the seeded-growth approach to tetrapod-shaped CdSe/CdTe nanocrystals.

absorbed across the whole visible spectrum, as photons can be absorbed either by the CdTe region or by the CdSe region, and in principle also by the intermediate states that exist as intraband processes[15–17] (the latter would render possible the absorption of photons carrying energies below the band gaps of both materials, which is important in photovoltaic applications). Additionally in this type of heterojunctions, the charge separation of electrons and holes at the interface between CdTe (behaving as electron donor) and CdSe (behaving as electron acceptor) occurs, leading therefore to localization of electrons in the CdSe region and holes in the CdTe region. Indeed, both theoretical and ultrafast electron-transfer-dynamics investigations in CdSe/CdTe donor–acceptor materials have demonstrated that type-II nanocrystal heterostructures induce charge separation and localize carriers to different regions of the heteromaterials.[25] Figure 2a shows the absorption spectra and molecular structures involved in the investigated photovoltaic cells. C60 and P3HT have complementary absorption spectra with high absorption coefficients, while the CdSe/CdTe tetrapods exhibit a broadband absorption covering the whole visible range up to 780 nm. Typical absorption spectra of CdSe seeds and corresponding CdSe/CdTe tetrapods are presented in Figure 2b (upper panel). The absorption of CdSe seeds exhibits a sharp peak around 550 nm. Upon growth of CdTe arms onto the CdSe seed, this peak is not seen any more, but new absorption features emerge, due mainly to absorption from the arms, which basically dominate the absorption spectrum. Although these heterostructures are type II, no evidence of type-II absorption is seen in these nanocrystals. In fact, the contribution of ''type-II'' absorption is probably negligible, because the contribution of the CdTe absorption is overwhelming.[26,27] These nanocrystals are therefore different from the recently reported type-II quantum dots and tetrapods,[18,26] which exhibit a distinctive sub-band-gap tail. Figure 2b (lower panel) shows the PL spectra of the CdSe seeds and that of

the final CdSe/CdTe tetrapods. The starting CdSe seeds exhibit a peak at 560 nm. After growth of CdTe arms, the PL of CdSe was not observed any more, and a new weak band appeared at around 730 nm, which can be attributed to band-edge emission from CdTe. The low-temperature PL spectrum recorded on CdSe/CdTe tetrapods and reported by us in our synthesis work[20] showed an additional PL emission peak in the infrared region (at around 950 nm), which corresponds to the type-II transition arising from the recombination of electrons localized in the CdSe seed with holes localized in the CdTe arms.

In order to exploit the photovoltaic properties of the CdSe/CdTe heterostructures, we first fabricated devices using a single-component spin-coated film of CdSe/CdTe tetrapods as photoactive layer. Figure 3a shows the current–voltage characteristics of a typical solar-cell device with structure of indium tin oxide (ITO)/poly(3,4-ethylenedioxythiophene) poly(styrenesulfonate) (PEDOT:PSS)/CdSe@CdTe/Al both under AM1.5G illumination and in the dark. The inset shows the energy diagram with the valence- and conduction-band levels for CdSe/CdTe tetrapods. The device exhibited an open-circuit voltage (V_{oc}) of 0.34V, short-circuit current density (J_{sc}) of 1.74 mA cm^{-2}, fill factor (FF) of 0.28, and power conversion efficiency (η) of 0.16% under AM1.5G illumination (100 mW cm^{-2}). These performances are improved with respect to those reported so far for similar all-nanocrystal devices based on CdTe/CdSe tetrapods,[19] and also higher than those reported for single-material devices based only on CdSe or CdTe nanocrystals.[1,19,23] However, absolute values for the power-conversion efficiency remain still low due to the small-scale heterostructures and to the electron trapping in the high-electron-affinity tetrapod CdSe cores. Additionally, as spin-coated films of tetrapods leave empty volumes when deposited into a film, thus determining non-optimized charge percolation paths to the electrodes, charges cannot easily move through the film once the excitons are separated. This suggests that optimization of the device composition, morphology, and annealing are needed, eventually by combining the nanocrystal heterostructures with organic compounds.

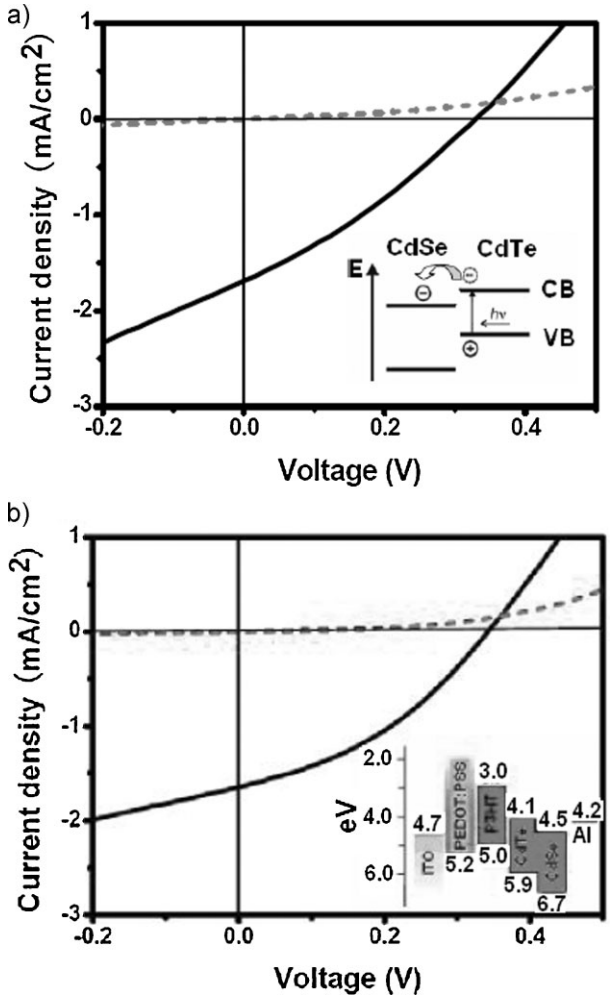

Figure 3. a) Current–voltage characteristics of PV cells with structure ITO/PEDOT–PSS/CdSe@CdTe/Al. The inset shows an energy diagram highlighting the valence and conduction band levels for CdSe@CdTe tetrapods. b) Current–voltage characteristics for PV cells with structure ITO/PEDOT–PSS/P3HT:CdSe@CdTe/Al under illumination (solid line) of one-sun AM 1.5G and in the dark (dash line). The inset shows a schematic energy band representation of the cell.

We have additionally fabricated and tested hybrid solar cells in which the active layer is a blend of P3HT and CdSe/CdTe tetrapods, acting as electron donor and acceptor, respectively. Indeed, in recent years photovoltaic cells based on nanocrystals blended with semiconducing polymers have achieved good power-conversion efficiency.[4–9] The growing interest in organic–inorganic hybrid devices is mainly due to the possibility of combining the low-cost thin-film fabrication of the polymers with good electrical and optical properties of the inorganic nanoparticles. Figure 3b shows the current–voltage characteristics of the hybrid photovoltaic device in the dark and under Am1.5G illumination, 100 mW cm^{-2}. The inset reports a schematic energy-band representation of all the materials involved in the device, showing a relative alignment of the energy levels[17,28] that allows for an efficient working of the cell. The J_{sc}, V_{oc}, and FF of the device are 1.68 mA cm^{-2}, 0.35 V, and 0.36, respectively, yielding a power conversion efficiency of 0.21%. Compared to the single-component-tetrapod devices discussed above, the efficiency is improved due to the good percolation pathway to the electrodes and to the increased fraction of light harvested by the combination of polymer and nanocrystals. Figure 1c shows the transmission electron microscopy (TEM) image of a hybrid blend film employing 89 wt% CdSe/CdTe tetrapods in P3HT. The substantial improvement of the morphological properties of the film is resulted from the deposition of the blend. The results indicate that these type-II CdSe/CdTe tetrapods are promising for applications in hybrid photovoltaic devices, even though at the present early stage of device optimization the efficiency is still low.

In order to optimize device performances and exploit the full potential of heterostructured tetrapod nanocrystals, we started from the consideration that two main types of PV structures are usually considered for hybrid cells: bulk heterojunctions and heterojunctions. The interpenetrating network structures have proven to be very efficient exciton-dissociation systems for bulk heterojunctions. On the other hand, heterojunctions are relatively simple systems, and materials can be characterized independently.[29] In our case, heterojunctions are well suited to

the investigation of new materials. Here, we demonstrate a new type of hybrid PV heterostructure device in which CdSe/CdTe tetrapods, differently from conventional approaches, act as electron-donor compounds. To this aim, we used good electron-conducting fullerene (C60) as interlayer material. Biebersdorf et al. have reported that C60 can be sensitized by electrons from photoexcited semiconductor NCs,[30,31] although photovoltaic properties were not investigated in that work. In this report, we fabricated a PV device by sequentially spin-coating a CdSe/CdTe film on ITO glass coated with 30 nm PEDOT:PSS and then evaporating a fullerene film onto it. A brief annealing of the CdSe/CdTe film for 20 min at 150 °C removed the residual solvent and allowed for subsequent deposition of the C60 film. In this way, a densely packed nanocrystal film covered with C60 was formed. The scanning electron microscopy (SEM) image in Figure 4a shows a homogeneous thin film of CdSe/CdTe tetrapods used for the photovoltaic cells. The inset shows a higher SEM magnification of such tetrapod film. The SEM image of Figure 4b shows tetrapod layers covered with C60, and a partial aggregation of C60 can be observed. A representative SEM image (Fig. 4c) of a cross-section of a 140-nm-thick film consisting of only tetrapods reveals that most tetrapods are close-packed. Figure 5a shows the PV cell structure based on a CdSe@CdTe/C60 active layer. The schematic energy diagram of Figure 5b illustrates the staggered band alignment,[17,28,31] and shows the charge separation and transport for each component material. Figure 5c shows current–voltage characteristics for PV cells with C60 interlayer device under illumination of one-sun AM 1.5 G, 100 mW cm^{-2} and in the dark. In the double-layer configuration with C60, we found promising cell performance. The J_{sc}, V_{oc}, and FF of the device are 3.15 mA cm^{-2}, 0.43 V, and 0.46, respectively, yielding a power conversion efficiency of 0.62%. Compared to the single-component tetrapod device and the hybrid P3HT–tetrapod device discussed above, the efficiency was significantly improved due to the presence of the C60 interlayer. We propose a mechanism for PV conversion based on D–A heterostructures. The CdSe/CdTe tetrapods function mainly as electron donors, and C60 works as acceptor and electron-transport interlayer in these PV cells. After light absorption and exciton formation, the majority holes in the CdSe/CdTe readily diffuse into ITO, whereas majority electrons in the C60 can diffuse toward the Al. Moreover, CdSe/CdTe-tetrapod heterostructures determine efficient internal charge separation. Electrons segregated in the CdSe cores in contact with C60 can diffuse through fullerene to the Al electrodes by virtue of the favorable energy-level alignment (see Fig. 5b). This allows for an increased charge collection and improved device performance. The proposed cell structure exploits the exciton-separation characteristics of CdSe/CdTe-tetrapod heterostructures for high-efficiency PV cells, demonstrating that electron localization in CdSe cores can be reduced by properly combining the nanocrystals with an organic compound acting as electron acceptor/transporting material, in our case C60. Finally, in our heterojunction cells this effect is limited to the interface, where C60 molecule and CdSe/CdTe are in contact, but the same scheme can be adopted for bulk-heterojunction cells, where complete electron collection can be obtained, thus allowing for further increase of device performance.

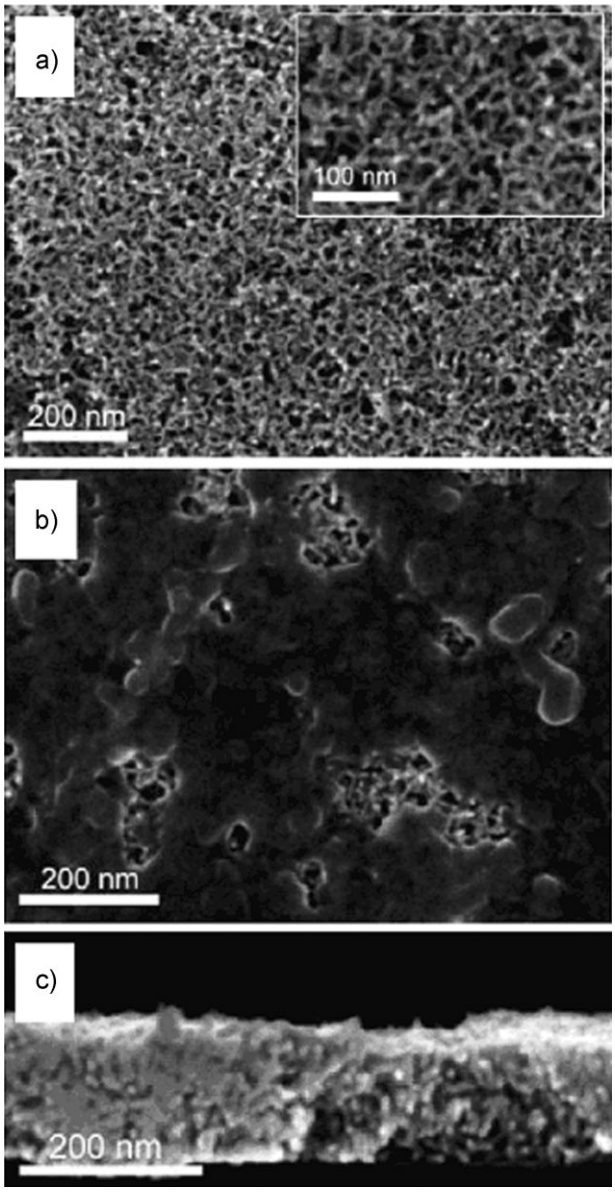

Figure 4. a) SEM image showing a homogeneous thin film of CdSe@CdTe tetrapods used in the photovoltaic cells. The inset represents a higher magnification of such thin film. b) SEM image showing tetrapod layers covered with C60 (a partial aggregation of C60 can be observed). c) SEM image of a cross-section of a 140-nm-thick film consisting only of tetrapods and revealing that most tetrapods are close-packed.

In conclusion, we report here PV devices embedding heterostructured tetrapod-shaped nanocrystals. In these nanocrystals, the arms were composed of CdTe and the central core was composed of CdSe, such that at the core/arm interface there is a type II band offset. Devices based on CdSe/CdTe–C60 active layers, in which the nanocrystal and Fullerene (C60) layers work as electron-donor and electron-acceptor/transport layers, respectively, were fabricated by exploiting the full potential of colloidal type-II tetrapod-nanocrystal heterostructures. Efficiencies up to 0.62% were reached in the hybrid cells. The PV performance was greatly improved with respect to that of CdSe/CdTe-P3HT- and

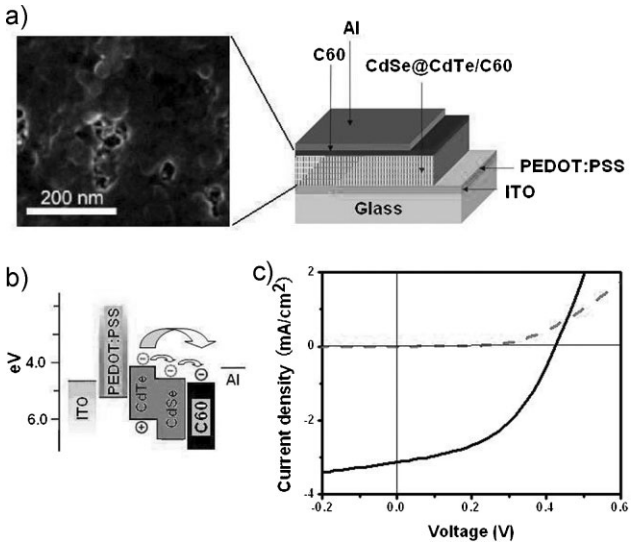

Figure 5. a) Schematic drawing of the PV-cell structure based on CdSe@CdTe/C60 active layer. Left: SEM image shows the active layer covered with C60. b) Energy-level diagram showing the charge separation and transport for each of the component materials. c) Current–voltage characteristics for PV cells with structure ITO/PEDOT-PSS/CdSe@CdTe/C60/Al under illumination of one-sun AM 1.5G (solid line) and in the dark (dash line).

CdSe/CdTe-based devices, fabricated as reference. The proposed approach provides a new general method for the fabrication of hybrid nanocrystal–C60 cells with a potentially long lifetime. We demonstrated the potential for the development of optimized organic–inorganic hybrid photovoltaic cells.

Experimental

Chemicals: Trioctylphosphine oxide (TOPO 99%), trioctylphosphine (TOP, 97%), cadmium stearate (90%), tellurium (Te, 99.999%), and selenium (Se, 99.99%) were purchased from Strem Chemicals. Octadecylphosphonic acid (ODPA, 99%) and hexylphosphonic acid (HPA, 99%) were purchased from Polycarbon Industries. Cadmium Oxide (CdO, 99.5%), 1-octadecene (ODE 90%), oleic acid (90%), oleylamine (70%), and anhydrous pyridine (99.8%) were purchased from Sigma–Aldrich. Regioregular poly(3-hexylthiophene-2,5-diyl) (P3HT) and fullerene-C60 (99.9%) were purchased from Sigma–Aldrich and used as received for device fabrication, without further purification. All solvents were anhydrous and were purchased from Sigma–Aldrich. A stock solution of Te:TOP (10 wt%) was prepared by adding 1 g of pure Te powder to a three neck flask containing 9 g of TOP and then heating at 320 °C under vigorous stirring and in nitrogen flow.

Synthesis: The CdSe/CdTe tetrapods were synthesized using the seeded-growth approach [20]. According to this method, the first step is to create the CdSe seeds with a spharelite structure, which allow the formation of tetrapods in the next step. For the synthesis of CdSe seeds, a mixture of 0.48 g (0.6 mmol) of cadmium stearate dissolved in 37 mL of 1-octadecene, prepared in a 100 mL three neck flask, was degassed under vacuum at 90 °C for 40 min. At this point, the solution was cooled to room temperature and 0.024 g (0.3 mmol) of Se powder were added to the solution under nitrogen flow, followed by degassing under vacuum for 10 min at 50 °C. After that the reaction mixture was heated and held for 3 min at 240 °C, a degassed solution of 0.1 mL of oleic acid and 1 mL of oleylamine in 4 mL of 1-octadecene was added drop-wise. After 1 h of growth, the reaction was stopped. For the purification, the CdSe seeds were precipitated with isopropanol, redissolved in toluene, reprecipitated with methanol, and finally dissolved in 1 mL of trioctylphosphine (TOP). To obtain CdSe/CdTe tetrapods, a 0.290 g octadecylphosphonic acid (ODPA), 0.080 g hexyl phosphonic acid (HPA), 3.000 g trioctylphosphine oxide (TOPO), 0.060 g cadmium oxide (CdO) mixture was loaded into a three-neck 50-mL flask, heated at 180 °C, and degassed for 40 min. After that the solution was cleared by heating to 340 °C, and 1.5 g of trioctylphosphine (TOP) was injected in the flask. When the temperature recovered to 340 °C, a solution of 0.6 g of Te in TOP (10 wt%) with 2.5×10^{-8} mol of CdSe seeds was injected. The reaction was stopped after 3 min, and the sample was cleaned by precipitating twice by adding methanol, centrifuging and redispersing in toluene. Often the as-synthesized heterostructures contained a small amount of by-products, such as nanorods. These could be separated from tetrapods by size- and shape-selective precipitation.

Pyridine treatment of the nanocrystals to remove the surfactant used in the synthesis of tetrapods was accomplished by dissolving the particles in anhydrous pyridine and stirring under reflux for 24 h. The nanocrystals were then precipitated with hexane and dissolved in a mixed solvent (chloroform: pyridine = 9: 1 vol/vol).

Photovoltaic Device: All manipulations were performed using standard air-free techniques. For single-component nanocrystal devices, highly concentrated solutions (60 mg mL^{-1}) of CdSe/CdTe tetrapods in pyridine–chloroform mixture solvent were used, while in hybrid polymer–nanocrystal devices, such solutions of CdSe/CdTe tetrapods were combined with solutions of P3HT in 1,2-dichlorobenzene. We chose the conjugated polymer P3HT as it has a high extinction coefficients in the visible region, high charge mobility, and excellent film processing ability, which leads to blended films with absorption covering the whole visible spectrum range from 380 to 750 nm. The solutions were spin-cast at 1500 rpm onto ITO-glass substrates coated with 30 nm PEDOT:PSS, and annealed on a hot plate at 150 °C for 20 min. For the hybrid CdSe/CdTe-C60 device, a 30 nm thick layer of C60, acting as electron-acceptor and electron-transport layer, was deposited by thermal evaporation at a pressure of 4.0×10^{-6} mbar (1 mbar = 100 Pa). Finally, the samples were held at $\sim 10^{-6}$ mbar overnight, after which aluminum top electrodes were deposited by thermal evaporation through a shadow mask, yielding eight individual devices with 0.08 cm^2 nominal area.

Characterization: Photoluminescence (PL) measurements were performed using a Varian Cary Eclipse fluorescence spectrophotometer with an intense xenon flash lamp. Absorption (Abs) measurements were carried out using a Cary 5000 UV-vis spectrophotometer. Low-magnification TEM images were recorded using a Jeol Jem 1011 microscope operated at 100 kV. The samples were prepared by dispersing dilute solutions of nanocrystals onto carbon-coated copper grids. Thin films of CdSe/CdTe-P3HT blends were investigated using TEM by casting a film on a KBr IR window, floating the film in water, and picking it up with a copper TEM grid. SEM images were obtained using the Scanning Electron Microscope FEI NOVAnanoSEM200. Typically, an accelerating voltage of 5 kV was used. Simulated AM1.5G illumination was realized with a Spectra Physics Oriel 150 W Solar Simulator with AM1.5G filter set. The integrated intensity was set to 100 mW cm^{-2} using a thermopile radiant power meter (Spectra Physics Oriel, model 70260) with fused-silica window. Current–voltage characteristics were carried out using the solar simulator and a Keithley 2400 Source Measure Unit. All the measurements were performed with a sample holder encapsulated in a glove box.

Received: April 21, 2009
Revised: May 12, 2009
Published online: June 24, 2009

[1] I. Gur, N. A. Fromer, M. L. Geier, A. P. Alivisatos, *Science* **2005**, *310*, 462.
[2] Y. Wu, C. Wadia, W. Ma, B. Sadtler, A. P. Alivisatos, *Nano Lett.* **2008**, *8*, 2551.

[3] B. Tian, X. Zheng, T. J. Kempa, Y. Fang, N. Yu, G. Yu, J. Huang, C. M. Lieber, *Nature* **2007**, *449*, 885.
[4] W. U. Huynh, J. J. Dittmer, A. P. Alivisatos, *Science* **2002**, *295*, 2425.
[5] I. Gur, N. A. Fromer, C. P. Chen, A. G. Kanaras, A. P. Alivisatos, *Nano Lett.* **2007**, *7*, 409.
[6] B. Sun, H. J. Snaith, A. S. Dhoot, S. Westenhoff, N. C. Greenham, *J. Appl. Phys.* **2005**, *97*, 014914.
[7] B. Sun, N. C. Greenham, *Phys. Chem. Chem. Phys.* **2006**, *8*, 3557.
[8] P. Wang, A. Abrusci, H. M. P. Wong, M. Svensson, M. R. Andersson, N. C. Greenham, *Nano Lett.* **2006**, *6*, 1789.
[9] W. J. E. Beek, M. M. Wienk, R. A. J. Janssen, *Adv. Mater.* **2004**, *16*, 1009.
[10] M. Grätzel, *J. Photochem. Photobiol. A* **2004**, *164*, 3.
[11] M. Law, L. E. Greene, J. C. Johnson, R. Saykally, P. D. Yang, *Nat. Mater.* **2005**, *4*, 455.
[12] A. P. Alivisatos, *J. Phys. Chem.* **1996**, *100*, 13226.
[13] C. B. Murray, C. R. Kagan, M. G. Bawendi, *Annu. Rev. Mater. Sci.* **2000**, *30*, 545.
[14] M. Shim, C. J. Wang, D. J. Norris, P. Guyot-Sionnest, *MRS Bull.* **2001**, *26*, 1005.
[15] D. Gross, A. S. Susha, T. A. Klar, E. D. Como, A. L. Rogach, J. Feldmann, *Nano Lett.* **2008**, *8*, 1482.
[16] S. Kumar, M. Jones, S. S. Lo, G. D. Scholes, *Small* **2007**, *3*, 1633.
[17] J. E. Halpert, V. J. Porter, J. P. Zimmer, M. G. Bawendi, *J. Am. Chem. Soc.* **2006**, *128*, 12590.
[18] S. Kim, B. Fisher, H. J. Eisler, M. G. Bawendi, *J. Am. Chem. Soc.* **2003**, *125*, 11466.
[19] H. Z. Zhong, Y. Zhou, Y. Yang, C. H. Yang, Y. F. Li, *J. Phys. Chem. C* **2007**, *111*, 6538.
[20] A. Fiore, R. Mastria, M. G. Lupo, G. Lanzani, C. Giannini, E. Carlino, G. Morello, M. D. Giorgi, Y. Q. Li, R. Cingolani, L. Manna, *J. Am. Chem. Soc.* **2009**, *131*, 2274.
[21] J. Kalinowski, G. Giro, N. Camaioni, V. Fattori, P. Di Marco, *Synth. Met.* **1996**, *77*, 181.
[22] J.-F. Nierengarten, T. Gu, T. Aernouts, W. Geens, J. Poortmans, G. Hadziioannou, D. Tsamouras, *Appl. Phys. A* **2004**, *79*, 47.
[23] T. Shiga, K. Takechi, T. Motohiro, *Sol. Energy Mater. Sol. Cells* **2006**, *90*, 1849.
[24] S. H. Wei, S. B. Zhang, A. Zunger, *J. Appl. Phys.* **2000**, *87*, 1304.
[25] C. J. Dooley, S. D. Dimitrov, T. Fiebig, *J. Phys. Chem. C* **2008**, *112*, 12074.
[26] D. J. Milliron, S. M. Hughes, Y. Cui, L. Manna, J. B. Li, L. W. Wang, A. P. Alivisatos, *Nature* **2004**, *430*, 190.
[27] D. Dorfs, T. Franzl, R. Osovsky, M. Brumer, E. Lifshitz, T. A. Klar, A. Eychmüller, *Small* **2008**, *4*, 1148.
[28] Y. Kim, M. Shin, I. Lee, H. Kim, S. Heutz, *Appl. Phys. Lett.* **2008**, *92*, 093306.
[29] Y. Shao, Y. Yang, *Adv. Mater.* **2005**, *17*, 2841.
[30] A. Biebersdorf, R. Dietmüller, A. Ohlinger, T. A. Klar, J. Feldmann, D. V. Talapin, H. Weller, *Appl. Phys. B* **2008**, *93*, 239.
[31] A. Biebersdorf, R. Dietmüller, A. S. Susha, A. L. Rogach, S. K. Poznyak, D. V. Talapin, H. Weller, T. A. Klar, J. Feldmann, *Nano Lett.* **2006**, *6*, 1559.